Test Bed for Vehicle Longitudinal Control Using Chassis Dynamometer and Virtual Reality: An Application to Adaptive Cruise Control

Mooncheol Won*, Sung Soo Kim, Byeong Bae Kang, Hyuck Jin Jung
Department of Mechatronics, Chungnam National University, Taejon 305-764, Korea

In this study, a test bed for vehicle longitudinal control is developed using a chassis dynamometer and real time 3-D graphics. The proposed test bed system consists of a chassis dynamometer on which test vehicle can run longitudinally, a video system that shows virtual driver view, and computers that control the test vehicle and realize the real time 3-D graphics. The purpose of the proposed system is to test vehicle longitudinal control and warning algorithms such as Adaptive Cruise Control(ACC), stop and go systems, and collision warning systems. For acceleration and deceleration situations which only need throttle movements, a vehicle longitudinal spacing control algorithm has been tested on the test bed. The spacing control algorithm has been designed based on sliding mode control and road grade estimation scheme which utilizes the vehicle engine torque map and gear shift information.

Key Words: ACC(Adaptive Cruise Control), Chassis Dynamometer, 3-D Real Time Graphics, Sliding Mode Control, ETC(Electronic Throttle Control), Estimation Algorithm

1. Introduction

A recent trend of automobile technology is to enhance safety and comport of drivers by adopting control systems having microprocessors, electronic sensors and actuators. In Adaptive Cruise Control(ACC) (Wiuner and Olbrich, 1998; Geduld, 1998), the throttle and the brake are controlled electronically by the aid of distance and velocity sensors, whereas the steering is done by the driver. An ACC vehicle can maintain relevant distance or velocity relative to the preceding vehicle using relative distance/velocity sensors. The system can reduce accidents by preventing human errors or achieving faster action than human in driving. Also the system can give comport to drivers by relieving the burden of handling the brake and the accelerator pedals.

In this study, a test bed for vehicle longitudinal control is developed using a chassis dynamometer and 3-D real time graphics(Fig. 6). In this test bed, a test vehicle can run longitudinally, and the 3-D graphics system realizes the virtual driver view for drivers. As a preliminary step before the real road tests, the test bed can be effectively used for developing both the control/warning algorithms and the hardwares for ACC, collision warning systems, and stop and go systems. With realistic 3-D graphics, it is also possible to evaluate human acceptance for control and warning algorithms. It is expected that the test bed is especially useful for testing of abnormal situations such as system faults and traffic accident situations.

The single roll chassis dynamometer with variable mechanical inertia is designed and manufactured using an eddy current dynamometer head. One interesting characteristic of the developed chassis dynamometer system is that the vehicle rear wheels, with the brake line attached, is pushed on the roller to realize the rolling resist-

* Corresponding Author,
E-mail : mcwon@cnu.ac.kr
TEL : +82-42-821-6875; **FAX** : +82-42-823-4919
Department of Mechatronics, Chungnam National University, Taejon 305-764, Korea.(Manuscript **Received** June 16, 2000; **Revised** March 9, 2001)

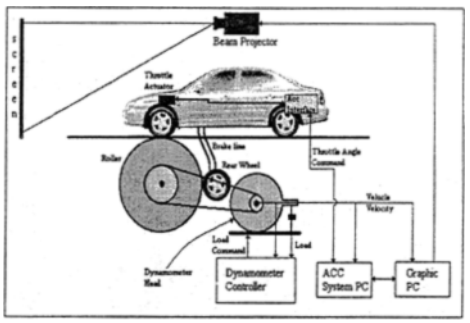

Fig. 1 Schematic diagram of test bed

ance and the brake force of the real wheel(choi and cho, 1998).

Based on sliding mode control, an ACC throttle control algorithm and an adaptation algorithm for road grade resistance are designed and verified on the developed test bed.

2. Test Bed for Longitudinal Control

2.1 Test bed system overview

The manufactured test bed system consists of a single roll chassis dynamometer and a real time three dimensional graphic system. The schematic diagram of the test bed is shown in Fig. 1. Figure 2 shows the actual test bed system.

The vehicle runs on the roller with a diameter of 1053 mm, which has a mechanically equivalent moment of inertia to the vehicle mass. Also, the vehicle rear wheels, with brake line attached, are pushed on the roller with a pressure equivalent to vehicle rear weight by pneumatic cylinders. The roller is connected with an eddy current dynamometer head by a timing belt. The dynamometer system can realize the loads to vehicle including aerodynamic and road grade resistances. From the encoder on the dynamometer axis, the real vehicle speed can be obtained.

A graphic PC generates the test scenarios and realizes the three dimensional real time graphics of roads and moving vehicles ahead. The ACC algorithms are implemerted on a notebook PC.

A medium size test vehicle with an automatic transmission is equipped with electrically controlled throttle system using a DC motor. The test

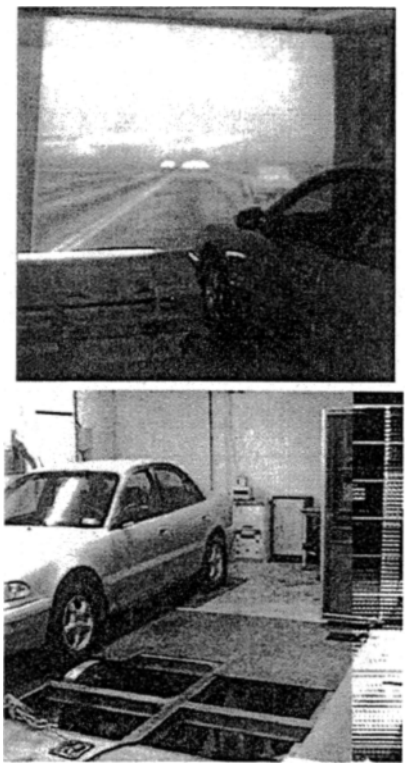

Fig. 2 Test bed system

vehicle does not have a relative distance/velocity sensor. The relative distance/velocity information is obtained from the prescribed position/velocity of the preceeding vehicle according to test scenarios and the measured test vehicle velocity and the numerically integrated vehicle position.

2.2 Vehicle load generation performance of chassis dynamometer

It is important to realize relevant load to the vehicle in the test bed, to match the test results on the roads and the test bed. Usually, coast down tests are performed to find the load. We carried out the coast down tests on roads having almost no road grade under relatively calm wind condition. We also performed the similar coast down tests on the test bed. Figure 3(a) shows the two test results. From the deceleration characteristics of the two tests, we can calculate the compensation load as a function of vehicle speed. Figure 3(b) compares the coast down test on the test bed with compensation load from the dynamometer with

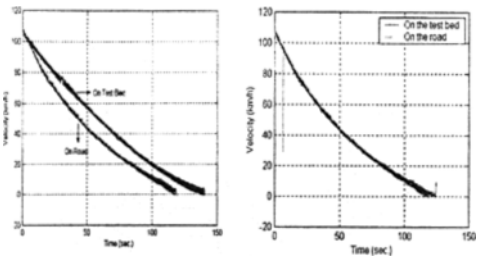

(a) Without load compensation (b) With load compensation

Fig. 3 Coast down test results on roads and test bed

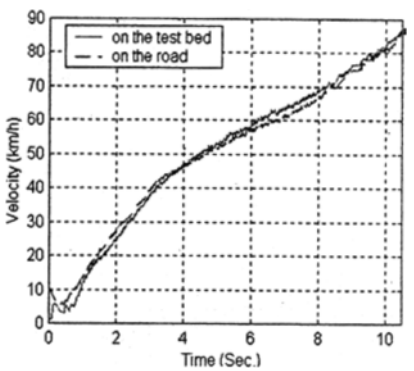

Fig. 4 Acceleration test results

the coast down test on the roads. The two results are almost identical. Also, vehicle acceleration tests has been done on both road and the test bed to verify the acceleration performance. We opened the throttle wide open(90 degrees) abruptly and maintained 90 degrees, and measured the vehicle velocity. Figure 4 shows the test results on the road and the test bed.

2.3 Virtual Reality Environment

In order to investigate the performance of the ACC controller and human acceptance of the proposed ACC controller on the proposed test bed, virtual reality environment has been established. To generate virtual reality environment, a graphic modeller 3D Studio Max(1999), a translator PolyTrans, and a scene generator OpenGVS(1998) have been employed. Figure 5 shows the procedure to generate virtual environment.

The 3D Studio Max has been used as a modelling tool to create geometric objects such as

Fig. 5 Procedure to generate virtual environment

(a) 3-D graphic scene

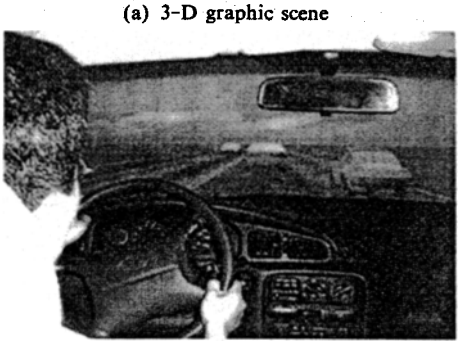

(b) Graphic scene inside the vehicle

Fig. 6 The created virtual environment for the ACC

car body, highway pavement and fields, etc. It also provides texture mapping capability to generate realistic object view. The created virtual environment from the 3D Studio Max has been exported to the OpenGVS by transforming 3D Studio Max format ".3ds" to OpenGVS format ".flt" using PolyTrans convertor. The OpenGVS is a high-level, Applications Programming Interface (API) for real-time 3D software developers and system integrators. It is also referred to as a scene management API. OpenGVS provides various API facilities such as scene, camera, channel, frame buffer, light source, fog model, and texture etc. for scene management. The created virtual environment for the ACC vehicle is shown in Fig. 6.

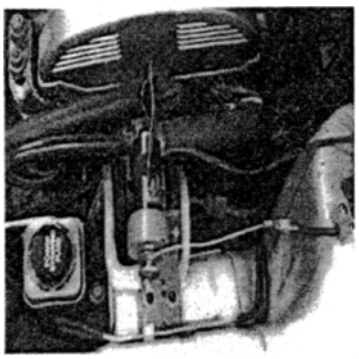

(a) DC motor connected to throttle

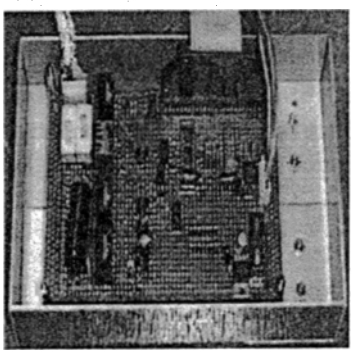

(b) DC motor driver

Fig. 7 Developed ETC system

3. Sensors and Actuator on Test Vehicle

3.1 Throttle actuator

Only a throttle actuator is now established on the test vehicle, a brake actuator will be added to the system in the future. On the test vehicle, an electric throttle actuator using a DC motor is attached to control throttle angle. Figure 7(a) shows the attached electric throttle control(ETC) system in the engine room without any change of existing throttle system., the DC motor is connected to throttle valve by a metal cable similar to a governor cable. If we turn off the power of the ETC system, we can also use the normal acceleration pedal. A compact 90 Watt, DC motor from Maxon motor is used. The motor uses 12 volt power from the battery in the vehicle. A traditional H-bridge motor driver is developed using MOSFET(Fig. 7(b)). There are various control strategies for DC motor driven throttle

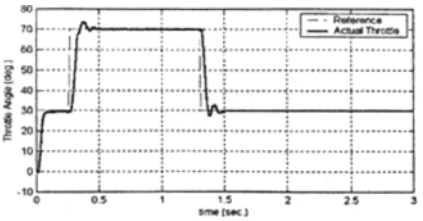

(a) Square wave tracking

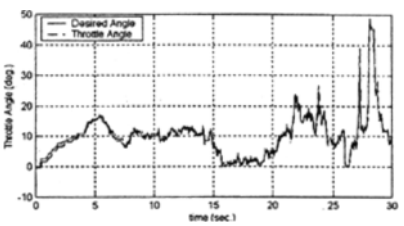

(b) Control command tracking

Fig. 8 Performance of ETC system

system(Jae-bok Song and Kyeong-seok Byeon, 1997). In this study, a simple PID plus feedforward control strategy is used and the feedback gains are scheduled. Figure 8 shows the performance of the developed electric throttle system. The steady state error is less than 0.5 degree, and the time to open the throttle from 0-90 degrees is about less than 70 msec.

3.2 Sensors used in the test vehicle

All the sensors used for the control are the production sensors, i. e., no additional sensors other than existing sensors in the vehicle are attached to realize the ACC system. The production throttle position sensor is used to measure the throttle angle. The engine speed is measured from the existing TDC(Top Dead Center)sensor. Gear position is also measured from the gear position command from TCU. Vehicle speed and torque converter turbine speed are obtained from the vehicle velocity sensor pickup attached on the transmission.

4. ACC Control Algorithm

An ACC throttle control algorithm based on sliding mode control is designed and verified on the test bed. Also, an estimation algorithm for road grade resistance is tested on the test bed.

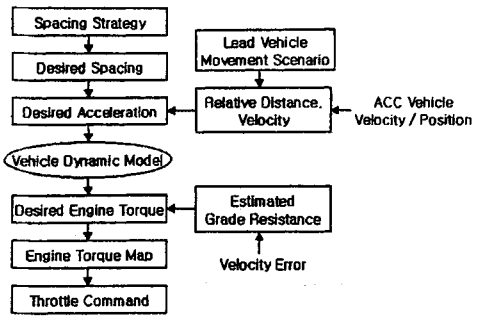

Fig. 9 Flow chart of control algorithm design

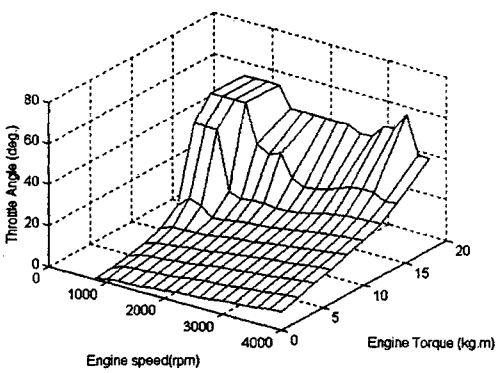

Fig. 10 $T_{net}(\omega_e, \alpha)$ Nonlinear function obtained from experiment

In this study the headway time control strategy is utilized to design the desired relative distance. The head way time is defined as a relative distance divided by the following vehicle speed. In designing the controller, the vehicle dynamics model including vehicle acceleration, engine, and torque converter model is utilized. Figure 9 shows the flow chart of control algorithm design process.

4.1 Longitudinal vehicle model

Engine acceleration model is represented as

$$J_{ep}\dot{\omega}_e = T_{net}(\omega_e, \alpha) - T_{pump} \tag{1}$$

where ω_e is engine speed, α is the throttle angle, J_{ep} is the effective inertia of engine and torque converter, T_{net} is the engine net torque, and T_{pump} is torque converter pump torque.

Steady state engine tests have been done to obtain the nonlinear engine torque map, T_{net} shown in Fig. 10.

Intake manifold dynamics of engine is neglected, since the dynamics is quite faster than the engine speed dynamics. A static torque converter model is used.

Vehicle longitudinal acceleration is obtained from the Newton's 2nd law.

$$\dot{x} = v \tag{2}$$

$$M_v\dot{v} = F_T - F_a - F_r - F_g \tag{3}$$

where x is vehicle position, v is vehicle velocity, M_v is the vehicle mass, F_a is aerodynamic drag, F_r is rolling resistance, F_g is road grade resistance, and F_T is the net force from tires.

4.2 ACC throttle control algorithm

According to the headway time strategy, the desired vehicle spacing, x_{r_des} is obtained from

$$x_{\_des} = v_f \cdot t_h \tag{4}$$

where v_f is the following ACC vehicle speed, and t_h is headway time.

The spacing error is defined as $e_s = x_{r\_des} - x_r$, where x_r is the vehicle spacing. When we have zero spacing error, we have $v_f t_h - x_r = 0$. Therefore, the desired vehicle velocity can be defined by

$$v_{f\_des} = \frac{x_r}{t_h} \tag{5}$$

We define the sliding surface or vehicle speed error as

$$s = v_{f\_des} - v_f \tag{6}$$

In this study, we design the sliding surface dynamics such that

$$\dot{s} = -\lambda\, Sat\left(\frac{S}{\Phi}\right) \tag{7}$$

where λ is a positive gain, and $Sat(\cdot)$ is defined by

$$Sat(x) = \begin{pmatrix} x, & |x| < 1 \\ 1, & x > 1 \\ -1, & x < -1 \end{pmatrix}$$

$Sat(\cdot)$ function is used to have better riding quality by preventing wild throttle movements, when initial velocity error is larger than the boundary layer thickness Φ. By differentiating the sliding surface, and using the notation, v_r, for the relative velocity, $\dot{x}_r$, we have

$$\dot{s}=\dot{v}_{f\_des}-\dot{v}_f=\frac{\dot{v}_r}{t_h}-\dot{v}_f=-\lambda\, Sat\left(\frac{s}{\Phi}\right) \tag{8}$$

Denoting $\dot{v}_f=a_{f\_des}$ in (8), the desired vehicle acceleration can be solved from (8)

$$a_{f\_des}=\frac{v_r}{t_h}+\lambda\, Sat\left(\frac{s}{\Phi}\right) \tag{9}$$

Now, we can calculate the desired engine torque using the vehicle dynamics model, and the desired vehicle acceleration. The necessary positive or negative tire force F_T to realize the desired acceleration is obtained from the vehicle dynamics model in (3).

$$F_T=M_v a_{f\_des}+F_r+F_a+F_g \tag{10}$$

The desired engine torque(T_{net_des}) can be calculated considering wheel inertia and transmission gear ratios.

$$T_{net\_des}=\frac{J_{eff}\dot{\omega}_{edes}+H_r\cdot r_{drive}\cdot r_{gear}(F_a+F_r+F_g)}{r_{tq}} \tag{11}$$

where H_r is the tire radius, r_{drive} is final drive gear ratio, r_{gear} is gear ratio, and r_{tq} is the torque ratio in the torque converter. Also, J_{eff} is the effective total inertia from the engine side, which can be expressed as follows

$$J_{eff}=(M_v\cdot H_r^2+J_w)\cdot r_{drive}^2\cdot r_{gear}^2+J_{ep} \tag{12}$$

where J_w is the wheel inertia. The desired engine acceleration, $\dot{\omega}_{edes}$, required to realize the desired vehicle acceleration, is given as

$$\dot{\omega}_{edes}=\frac{\dot{v}_{f\_des}}{H_r\cdot r_{drive}\cdot r_{gear}} \tag{13}$$

Therefore, the desired engine torque is expressed as

$$T_{net\_des}=\left[J_{eff}\cdot\left(\frac{\dot{v}_{f\_des}}{H_r\cdot r_{drive}\cdot r_{gear}}\right)+H_r\cdot r_{drive}\cdot r_{gear}(F_a+F_r+F_g)\right]/r_{tq} \tag{14}$$

The sum of aerodynamic resistance(F_a) and rolling resistance(F_r) can be obtained from the coast down test result as a function of the vehicle speed. Finally, the desired throttle angle, α_{des}, is obtained from the engine torque map.

$$\alpha_{des}=T_{net}^{-1}(\omega,\ T_{net\_des}) \tag{15}$$

4.3 Algorithm for estimating grade resistance

When the vehicle runs on road, the road grade is unknown. However, the road grade resistance can be too big to be compensated with the feedback gain λ. If we use too much gain value to overcome the road grade resistance, the ride quality can be degraded because of wild throttle movements. We can consider the road grade resistance as a time varying disturbance. Also, the wind resistance can be considered as an unknown disturbance. In this study, we use a disturbance adaptation algorithm to estimate those disturbances. The discrete-time disturbance adaptation and control law developed in (Won et al., 1994) can be applied to SISO feedback linearizable nonlinear systems with matched disturbance. When we apply the disturbance adaptation law in (Won et al., 1994) to this problem, the desired engine torque must be modified to

$$T_{net\_des}=\frac{J_{eff}\dot{\omega}_{edes}+H_r\cdot r_{drive}\cdot r_{gear}(F_a+F_r+\hat{F}_g)}{r_{tq}} \tag{16}$$

The only change is that F_g is replaced by $\hat{F}_g$, which is the estimated value of F_g.

The disturbance adaptation law in the discrete-time form is given as

$$\hat{F}_g(k+1)=\hat{F}_g(k)-M_v\lambda(k)(g_1(k)s(k+1)+g_2(k)s(k)) \tag{17}$$

where $s(k)$ is the sampled sliding surface i. e, vehicle speed error in (6).

Also, $\lambda(k)$, $g_1(k)$ and $g_2(k)$ are given as follows.

$$\lambda(k)=\begin{cases}\lambda & \text{for } |s(k)|\le\Phi\\ \dfrac{\lambda}{|s(k)|} & \text{for } |s(k)|>\Phi\end{cases} \tag{18}$$

$$g_1(k)=\begin{cases}g_1 & \text{for } |s(k)|\le\Phi\\ g_1|s(k)| & \text{for } |s(k)|>\Phi\end{cases} \tag{19}$$

$$g_2(k)=-g_1(k)(1-\lambda(k)t_s) \tag{20}$$

Here, t_s is the sampling period, λ is the same feedback gain in (7), and g_1 is a positive constant satisfying the following condition,

$$|1-\lambda g_1 t_s|<1 \tag{21}$$

he disturbance adaptation algorithm has

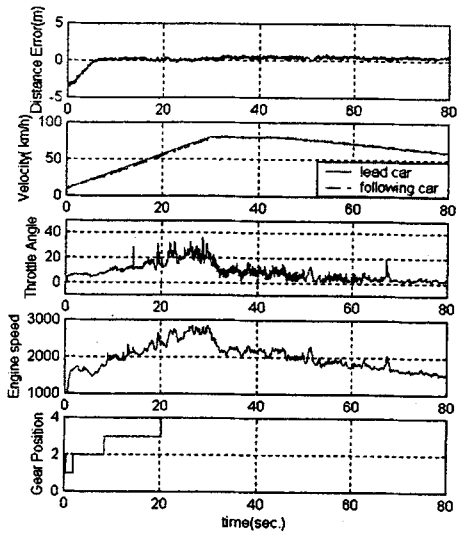

Fig. 11 ACC Test Result Without Road Grade Figure(Acceleration and Deceleration Velocity Profile)

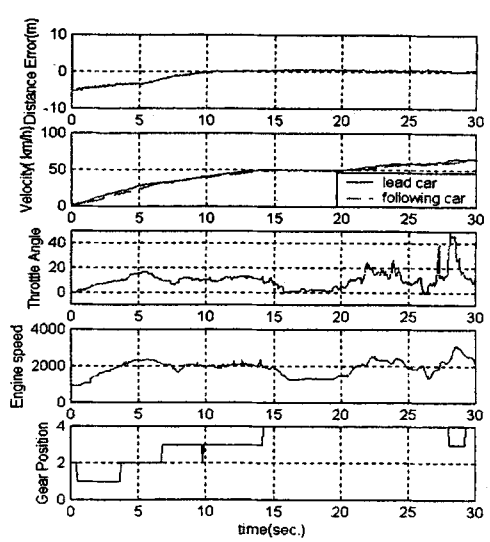

Fig. 12 ACC Test Result Without Road Grade(An Urban Road Driving Velocity Profile)

advantages over the conventional adaptive sliding mode control(Slotin and Li, 1991) in that disturbance adaptation or estimation is not affected by the tracking error (the velocity error, s, in this study) and input saturation.

5. Experimental Results

Since our test vehicle is not equipped with a brake actuator, the lead vehicle velocity profiles are selected such that the deceleration of the lead vehicle is not big.

The head way time(t_h) is fixed to 1.0 second, and the feedback gain(λ) is fixed to 0.3. The adaptation gain(g_1) is chosen as 1.0. The sampling time(t_s) is 10 msec, and the boundary layer thickness(Φ) is chosen as 1. 0m. The initial spacing errors are around -4 to -6 meters, which means the ACC vehicle must accelerate to maintain the desired spacing.

Figures 11 and 12 show the experimental results without grade resistance estimation. In those cases, the loads due to road grade are not applied to the vehicle, and the controller also assumes that the grade resistance is zero. From Fig. 11, we can see that the lead vehicle accelerates with a constant acceleration, and maintains a constant speed(80 Km/h) for a short period of time and finally decelerates with a constant deceleration. In this case, we can observed that the distance error is decreasing quickly within 5.0 seconds and maintained less than 0.7 m. In the next experiment without grade resistance estimation, the lead vehicle velocity profile is acquired from a real urban road driving. In this case, the tracking error is also maintained within 0.7m.

Figures 13 and 14 show the experimental results with grade resistance estimations. The last sub-figures show the estimation results. Figure 13 shows the case when the grade resistance changed from 750 N to 100 N at t=37.0 sec. The resistance of 750 N correspond to 3.0 degree road grade for the test vehicle of 1450 Kg mass. It takes 3~4 seconds to catch up the step change of grade resistance. The estimation performance seems to be acceptable from the point of distance error degradation due to the change of the grade resistance near t=37.0 sec. Figure 14 shows another road grade estimation result. In this case, the grade resistance is changed from 100 N to 500 N at t= 21.0 sec. We can see that the estimation

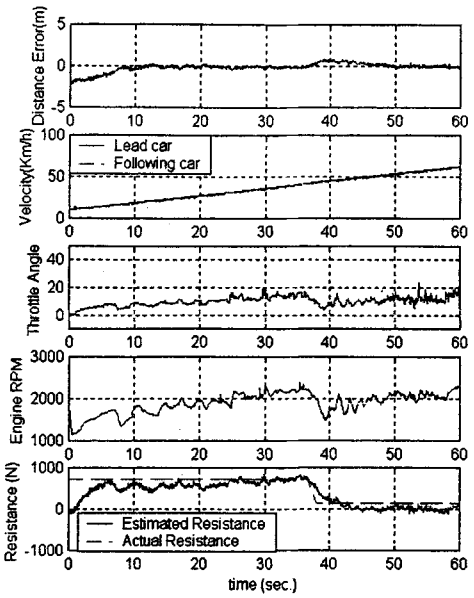

Fig. 13 ACC Test Result With Road Grade Estimation(Constant Acceleration Velocity Profile)

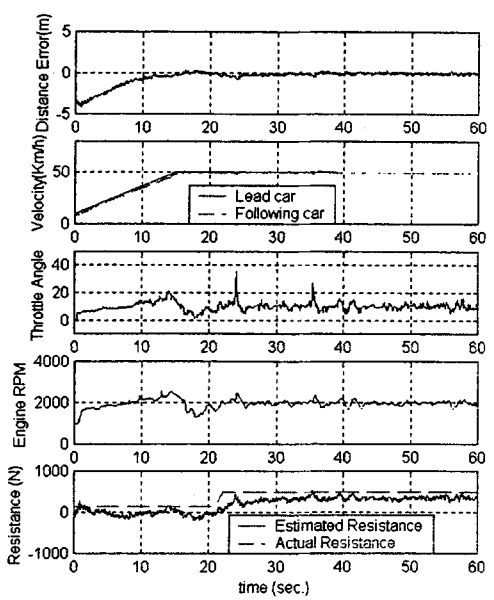

Fig. 14 ACC Test Result With Road Grade Estimation(Constant Acceleration and Constant Velocity Profile)

shows some steady state error. The steady state error can be induced from the model error of the engine torque map. In other words, the total uncertainty to be estimated is the sum the grade resistance and the error of engine torque map.

6. Conclusions

In this study, a test bed for vehicle longitudinal control is developed using a chassis dynamometer and real time 3-D graphics. On the test bed, a test vehicle with longitudinal control or warning facilities can run longitudinally, and a driver can experience the virtual reality 3-D graphic scenes. The performance of the chassis dynamometer is verified through the coast down tests and acceleration tests on the roads and the test bed. An ACC throttle control algorithm based on sliding mode control is designed using a vehicle dynamics model. Also, an estimation algorithm for road grade resistance is suggested. The control and estimation algorithms are verified on the test bed using a medium size test vehicle equipped with an electric throttle system. The experimental results show spacing error less than 1. 0 m. In the future work, a brake actuator will be added on the test vehicle, and more extensive tests will be performed.

References

Winner, H., and Olbrich, H., 1998, "Major Design Parameters of Adaptive Cruise Control," *AVEC'98*, pp. 723~728.

Geduld, G. O., 1998, "Collision Avoidance, Adaptive Cruise Control : Two Similar Application With Different Kinds of Philosophy and Safety Impact," AVEC'98, pp. 707~709.

Choi, S., and Cho, D. W., 1998, "Control of Wheel Slip Ratio Using Sliding Mode Controller with Pulse Width Modulation," *AVEC'98*, pp. 629~635.

Won, M., Choi, S., and Hedrick, J. K., 1994, "An Adaptive Sliding Mode Control of Automobile Engine Speed Under Unknown Loads," *1994 ASME Winter Annual Meeting* (Transportation Systems pp. 175~188).

Slotin, J. E., and Li, W., *Applied Nonlinear Control*, Prentice-Hall 1991.

OpenGVS Programming Guide Version 4.2, 1998, Gemini Technology Corporation and

Quantaum 3D. Inc. Lake Forest , CA, U. S. A.

3D Studio Max, reference manual Release 3, AutoDesk, Inc. Sau Rafael, CA, U. S. A., 1999.

Jae-bok Song and Kyeong-Seok Byeon, 1997, "Control of Throttle Actuator System Based on Time Delay Control," *Transactions of the KSME*, Vol. 21, No. 12, pp.